Supporting Information File

Dehydrogenation of amines in aryl-amine functionalized pincer-like nitrogen-donor redox non-innocent ligands *via* ligand reduction on Ni(II) template

Manas Khatua,[b] Bappaditya Goswami,[b] and Subhas Samanta*[a]

[b]Department of Chemical Sciences, Indian Institute of Science Education and Research Kolkata, Mohanpur-741246

[a]Department of Chemistry, Indian Institute of Technology Jammu, Jammu, India- 181221

Table of Contents

List of Table		
Table S1	Crystallographic Data Table of the complexes **2, 8**, **10** and **12**	**S29**

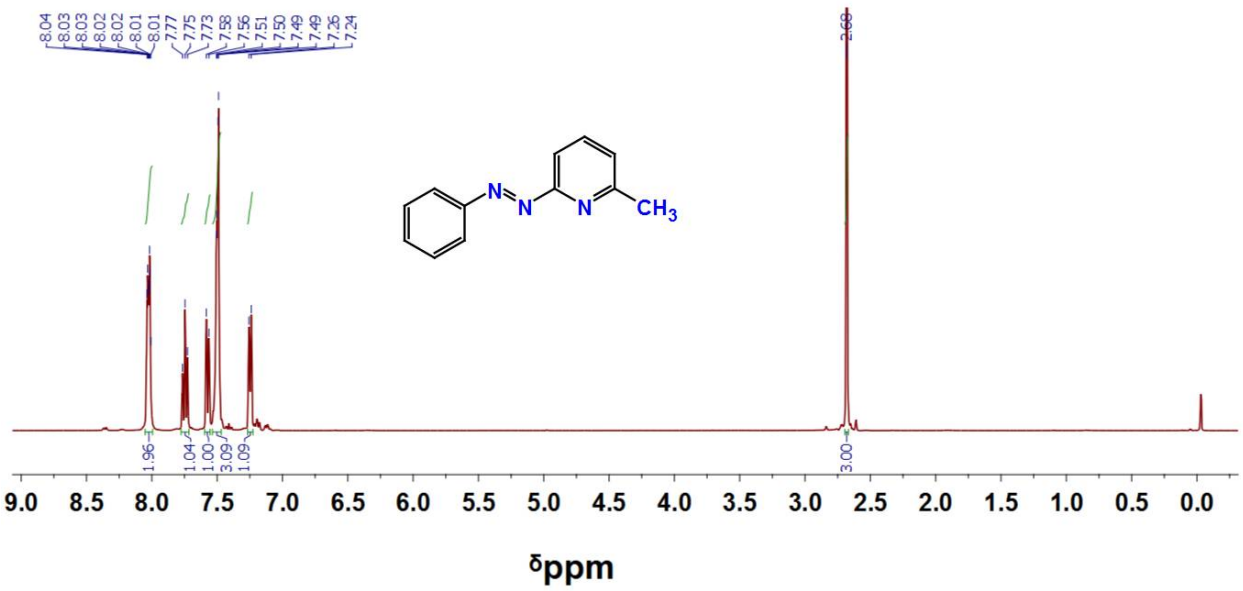

Figure S1. ^{1}H NMR Spectrum of compound **A** in $CDCl_3$

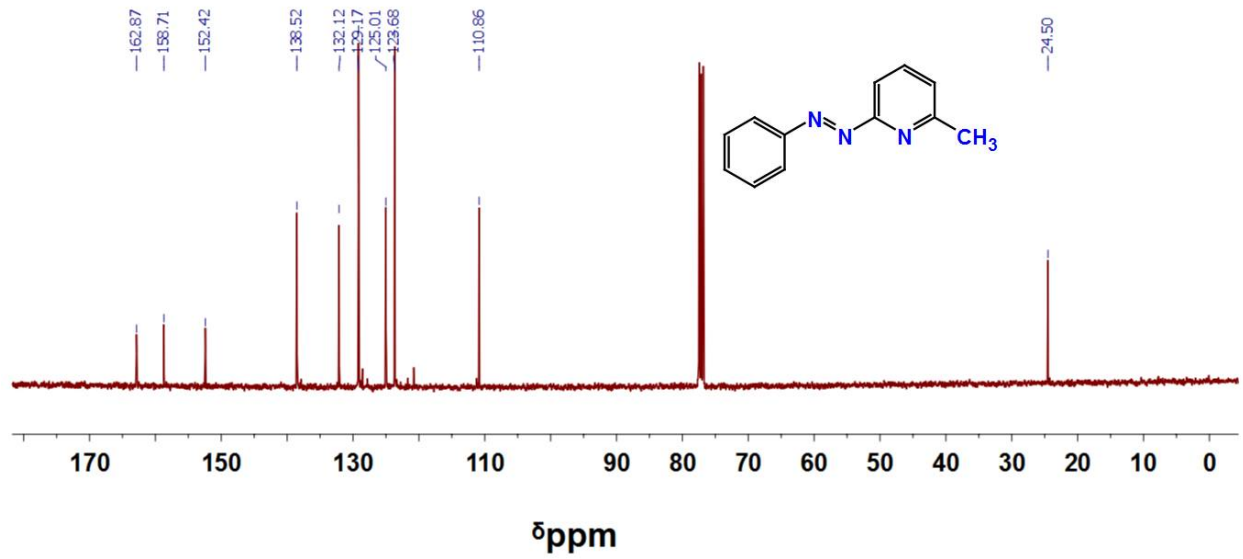

Figure S2. ^{13}C NMR Spectrum of compound **A** in $CDCl_3$

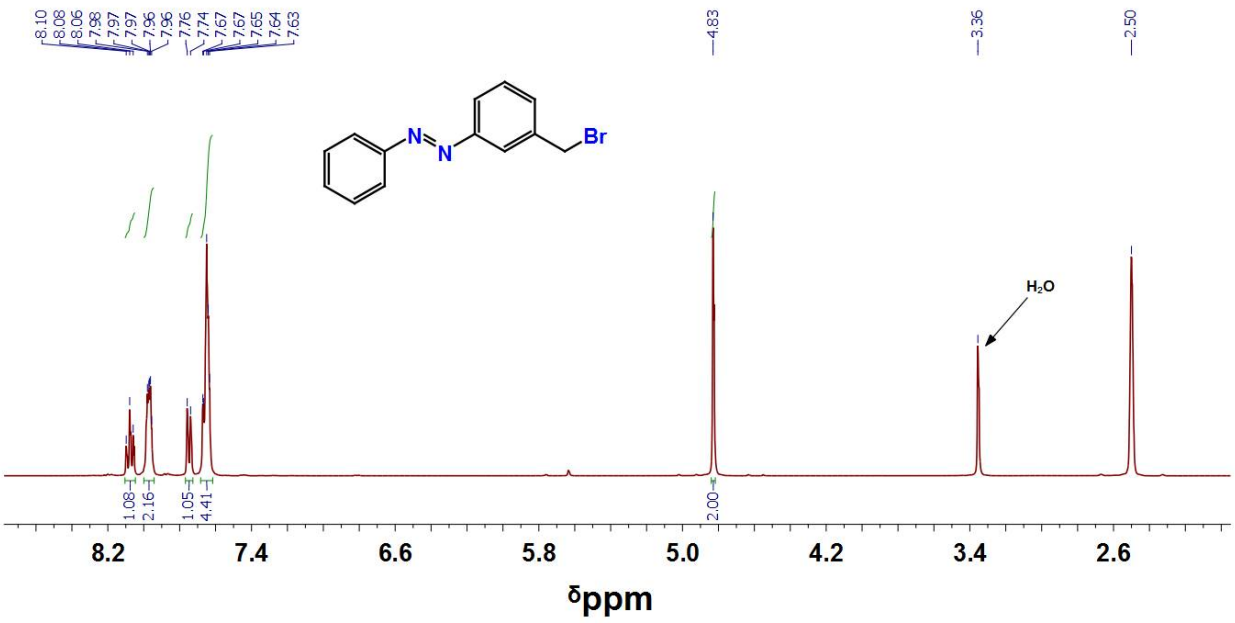

Figure S3. ^{1}H NMR Spectrum of compound **B** in d_6-DMSO

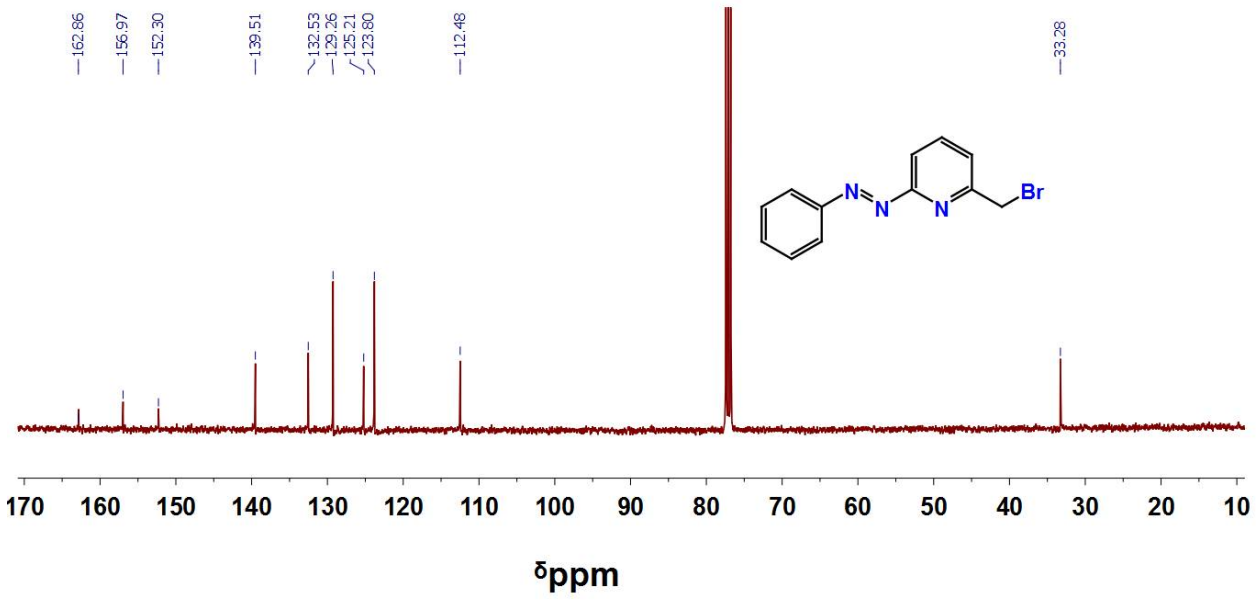

Figure S4. ^{13}C NMR Spectrum of compound **B** in $CDCl_3$

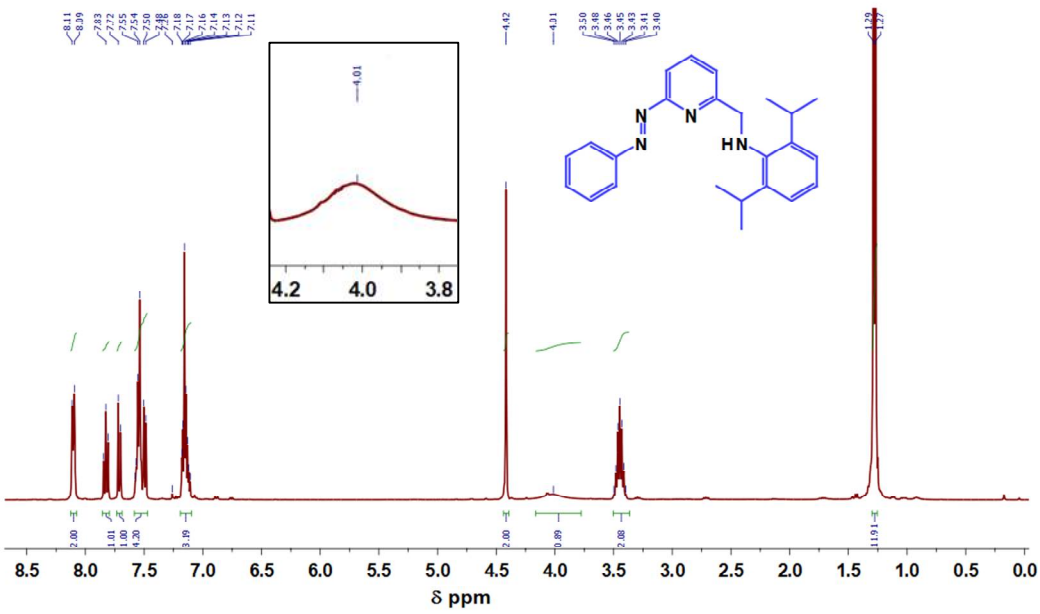

Figure S5. ^{1}H NMR Spectrum of **HL^{a}** in $CDCl_3$ [N-H proton shown in inset]

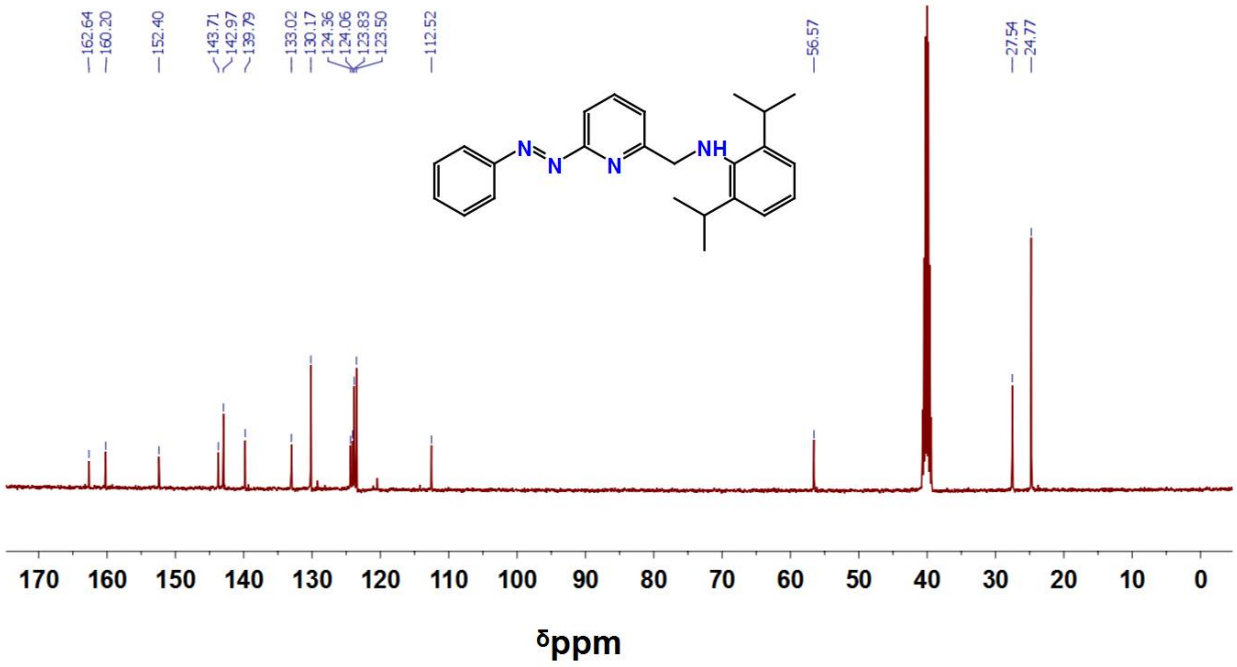

Figure S6. ^{13}C NMR Spectrum of **HL^{a}** in d_6-DMSO

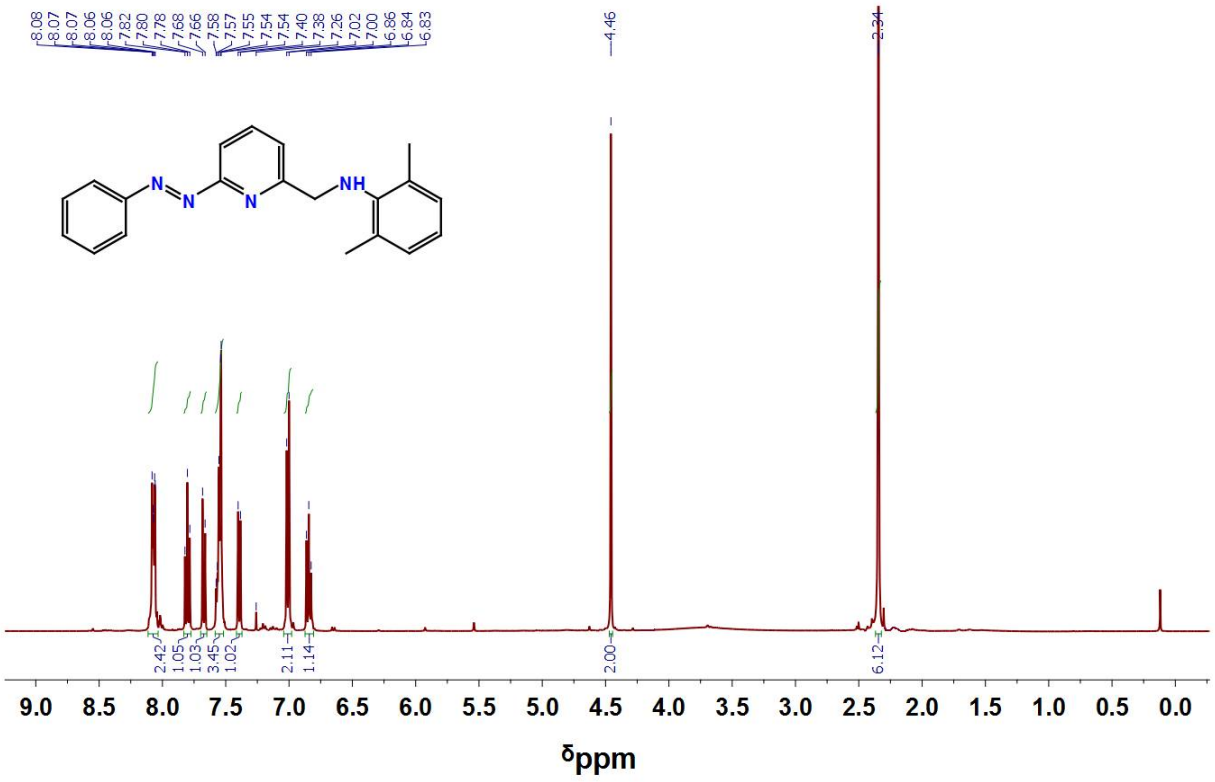

Figure S7. ^{1}H NMR Spectrum of **HL^{b}** in $CDCl_3$

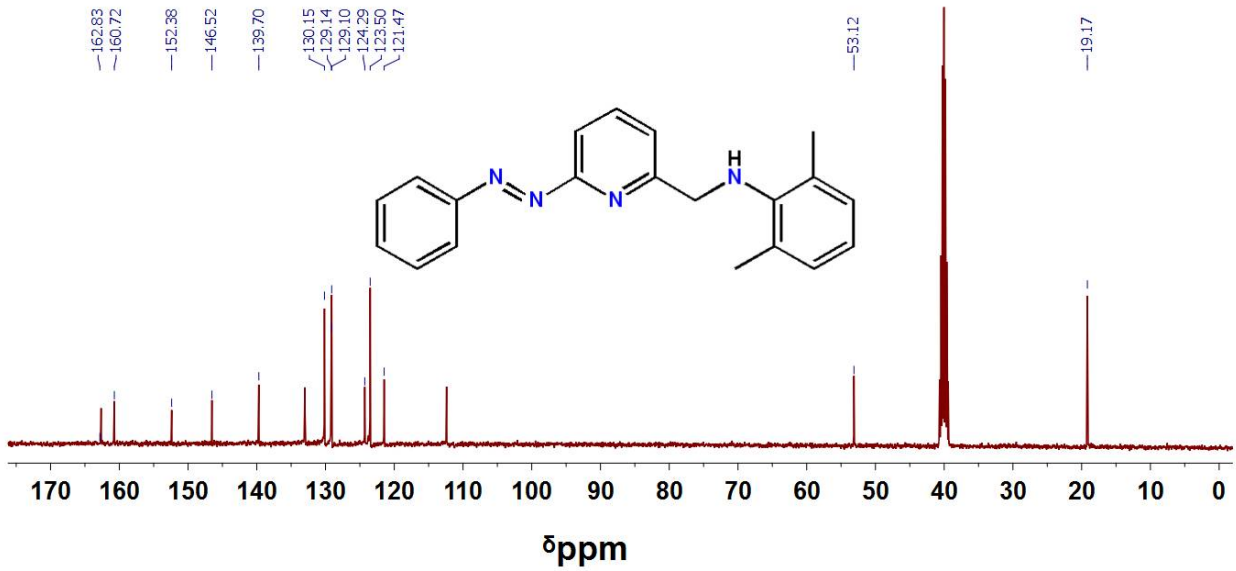

Figure S8. ^{13}C NMR Spectrum of **HL^{b}** in d_6-DMSO

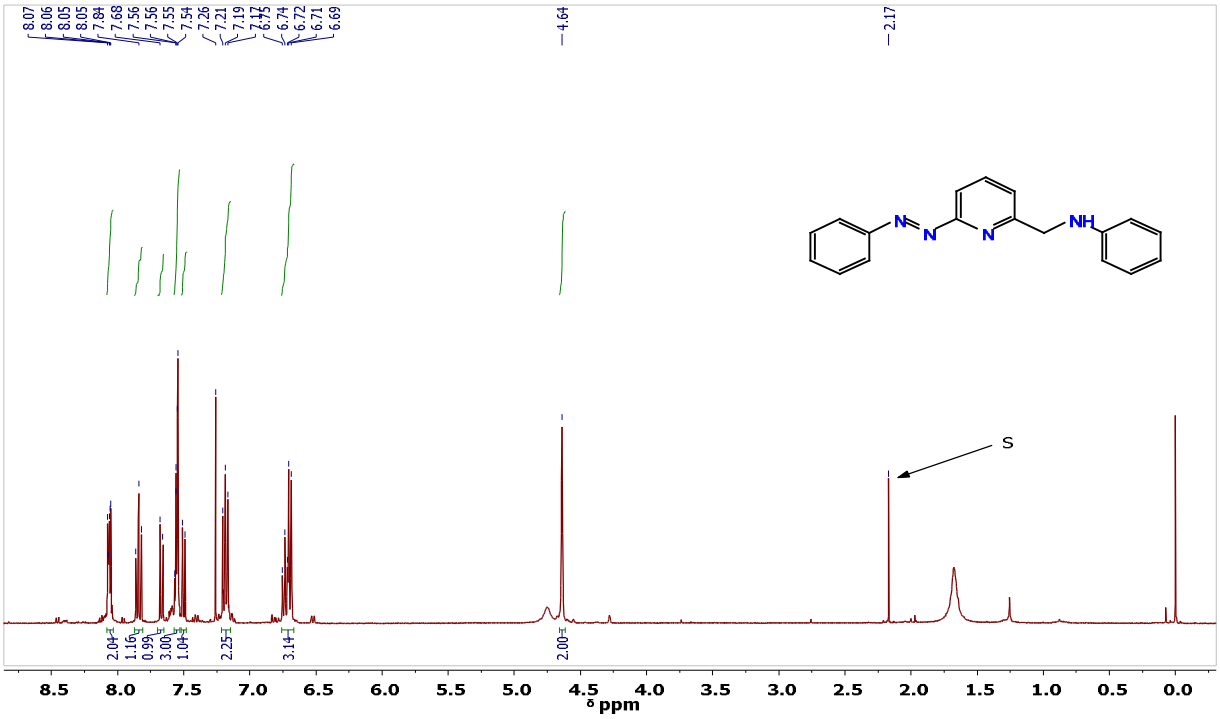

Figure S9. ^{1}H NMR Spectrum of **HL^{c}** in $CDCl_3$(s-acetone)

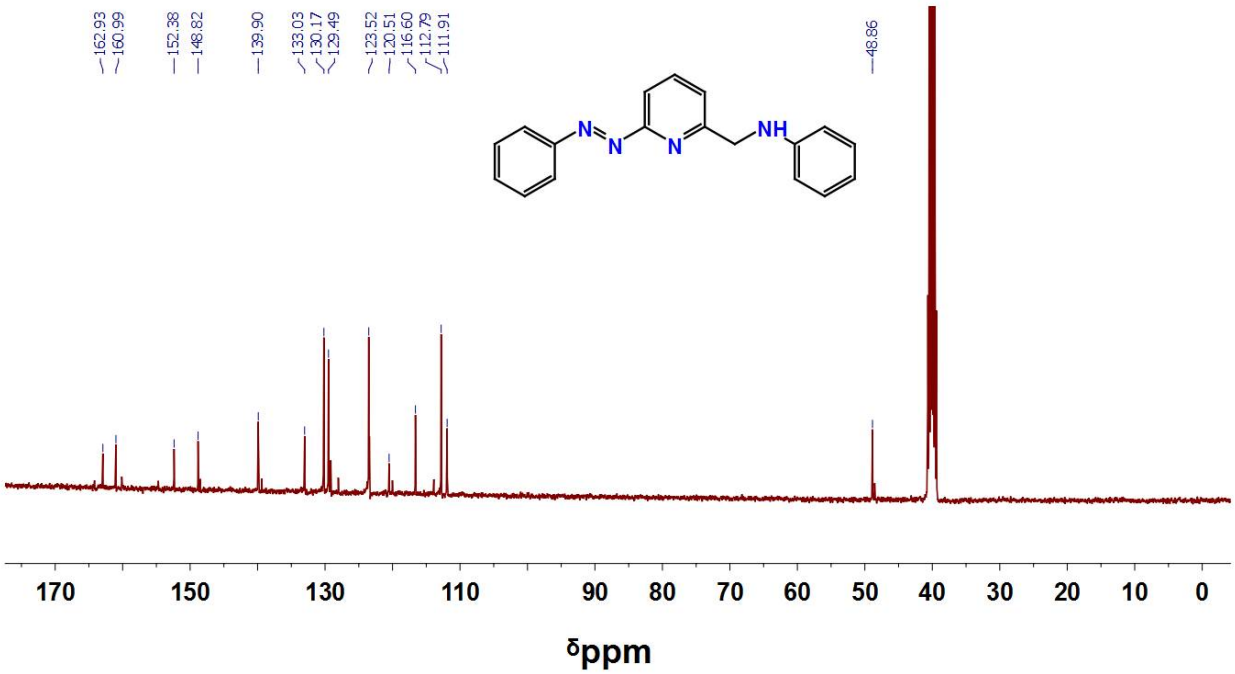

Figure S10. ^{13}C NMR Spectrum of **HL^{c}** in d_6-DMSO

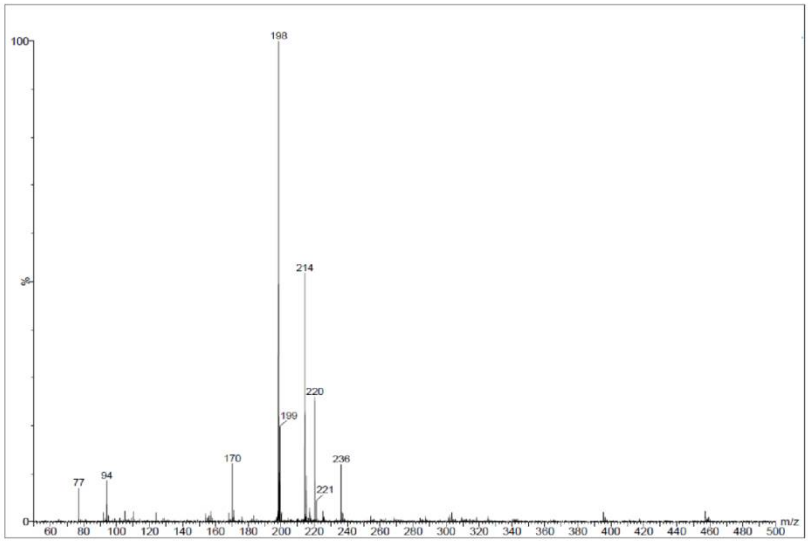

Figure S11. Full-range ESI-MS spectrum of the Compound **A** in acetonitrile

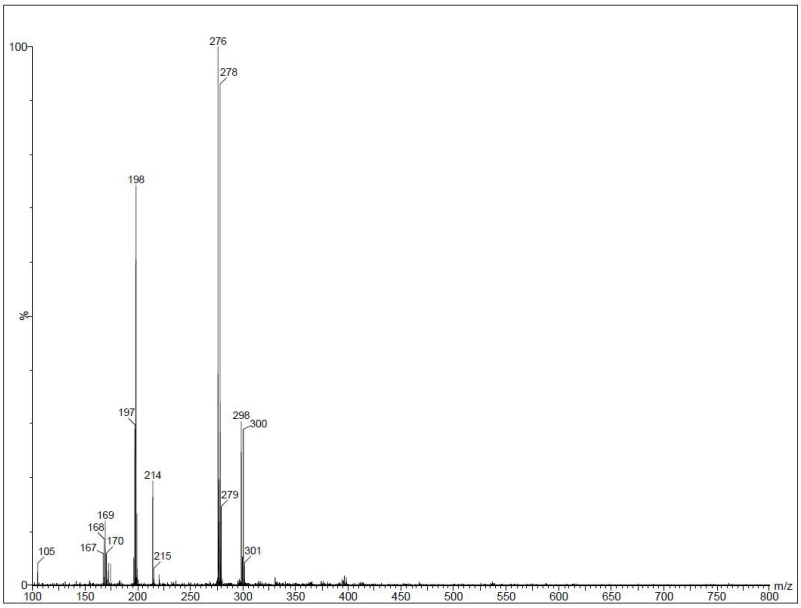

Figure S12. Full-range ESI-MS spectrum of Compound **B** in acetonitrile

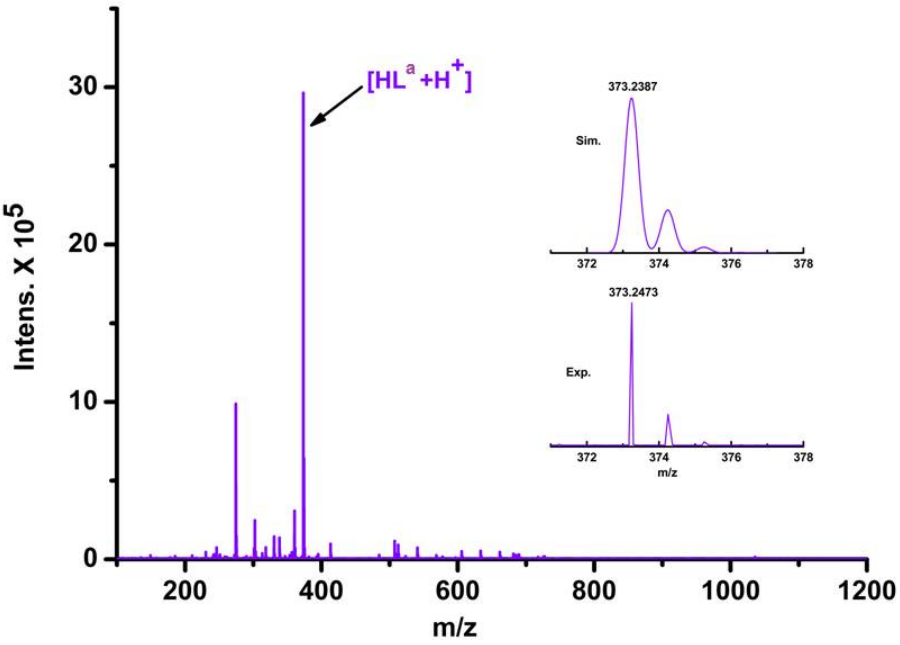

Figure S13. Full-range ESI-MS spectrum of the ligand **HL^a**

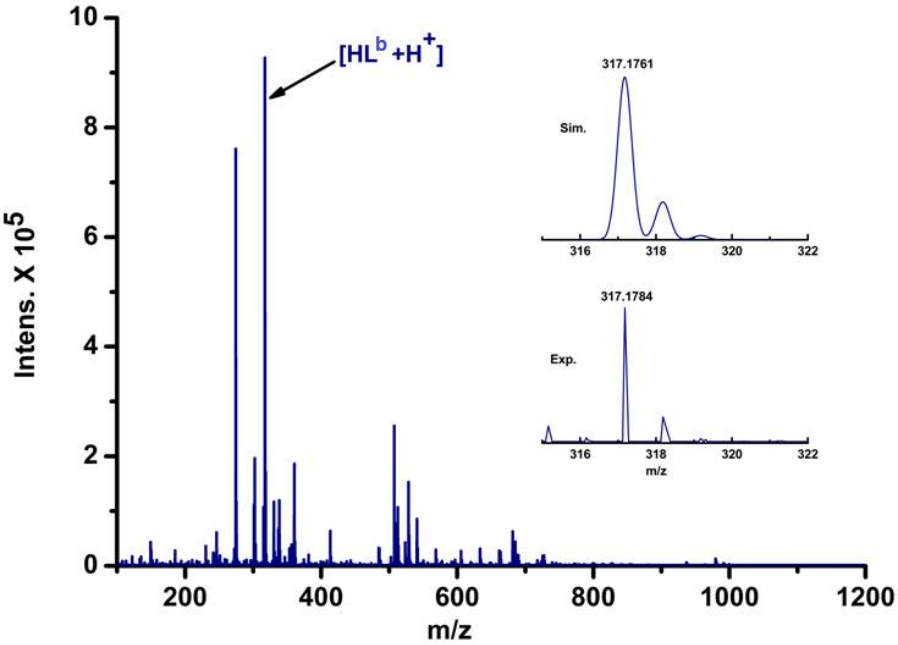

Figure S14. Full-range ESI-MS spectrum of the ligand **HL^b**

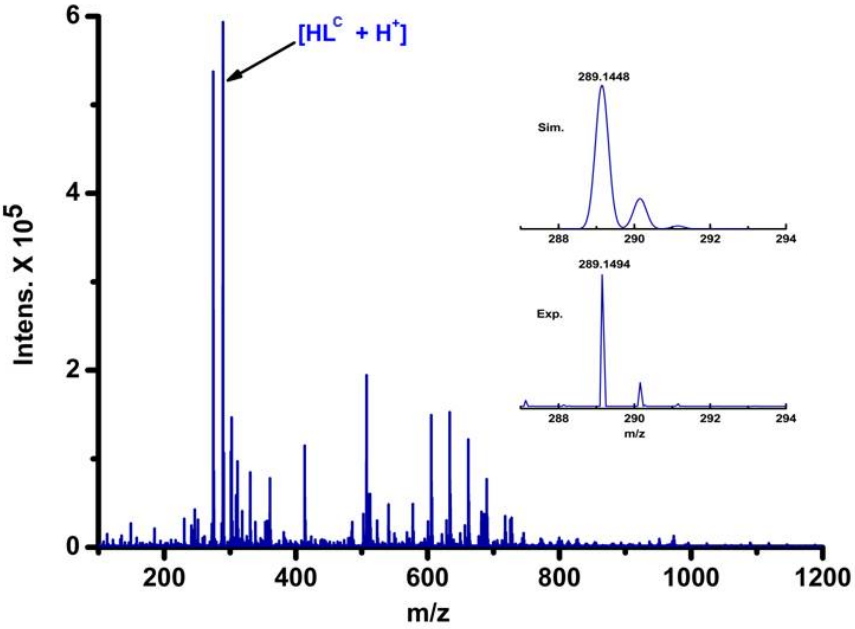

Figure S15. Full-range ESI-MS spectrum of the ligand **HL^c**

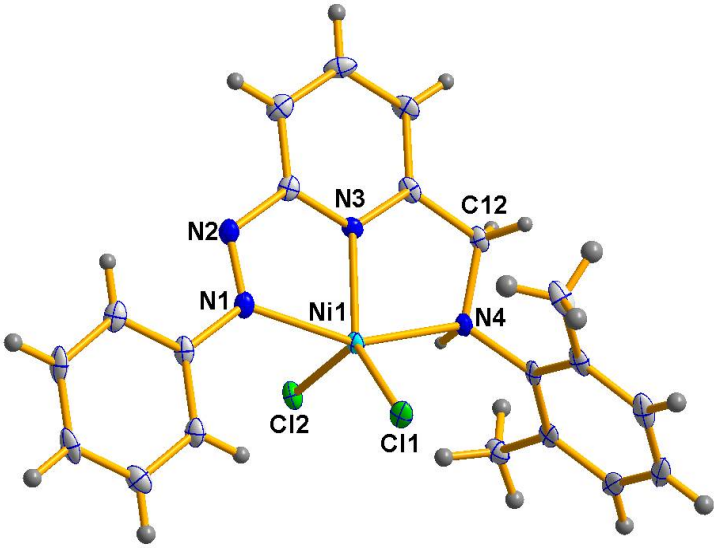

Figure S16. ORTEP representation and atom numbering schemes for the complex **2** in 50% probability level

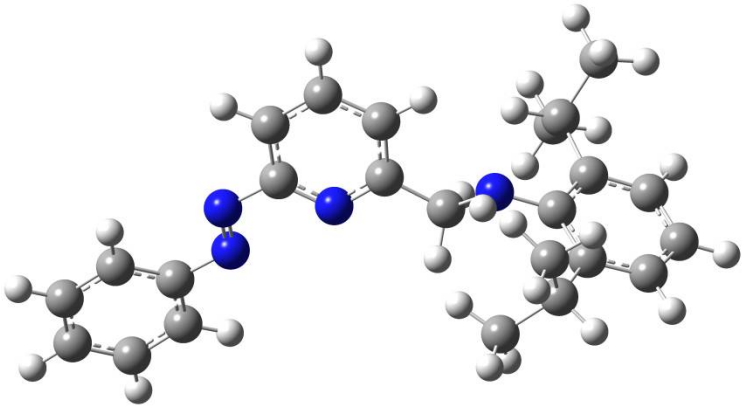

Figure S17. Optimized structure of the ligand **HL**[a]

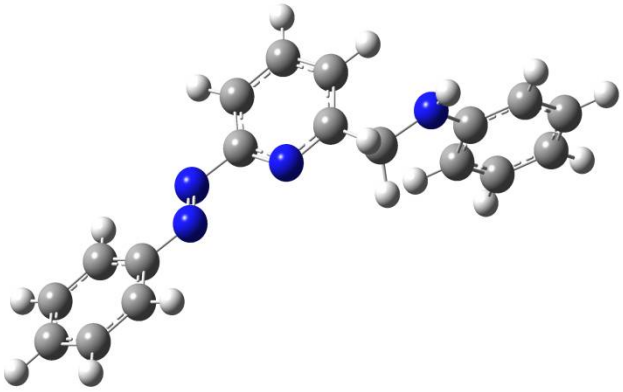

Figure S18. Optimized structure of the ligand **HL**[c]

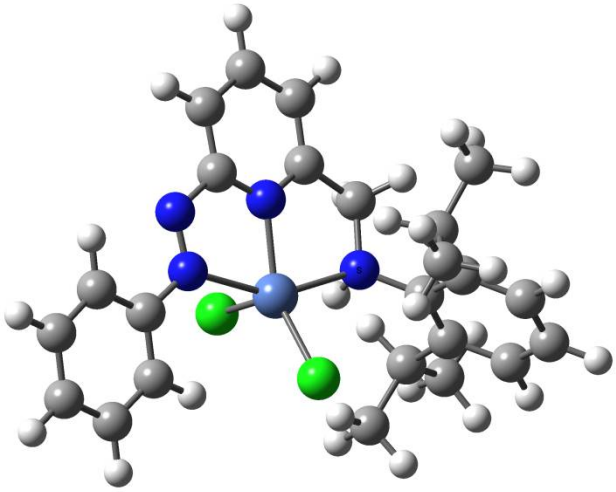

Figure S19. Optimized structure of the complex **1**

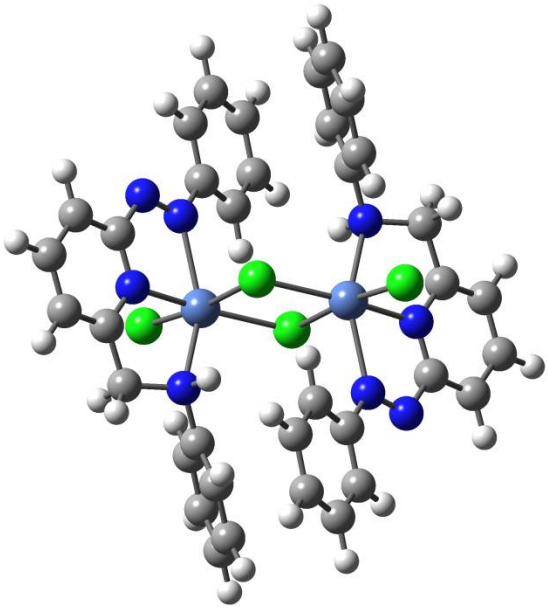

Figure S20. Optimized structure of the complex **3**

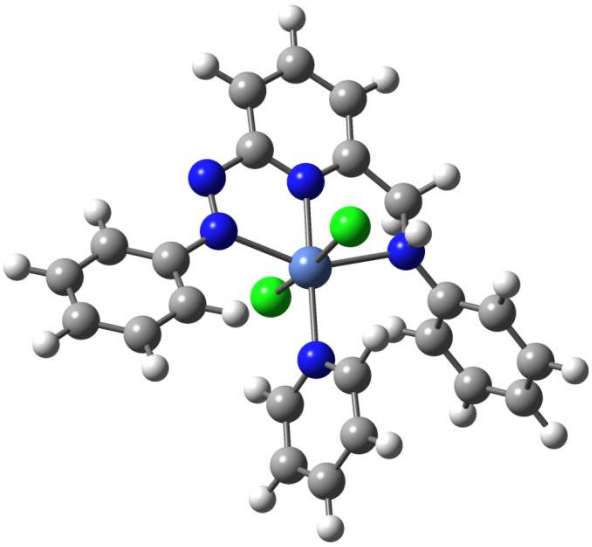

Figure S21. Optimized structure of the complex **6**

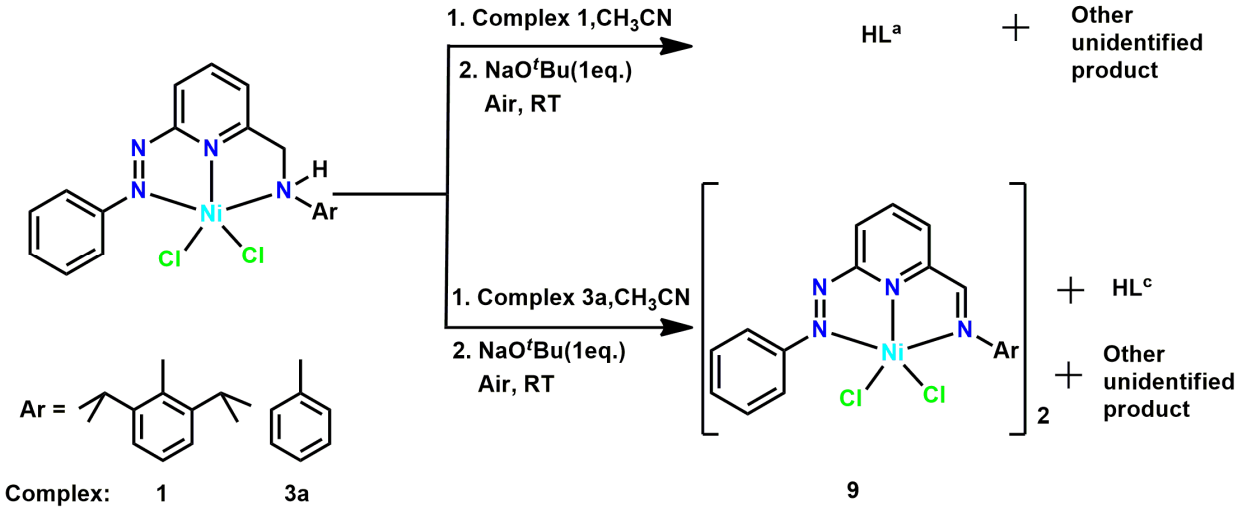

Figure S22. Reaction with NaO^{t}Bu

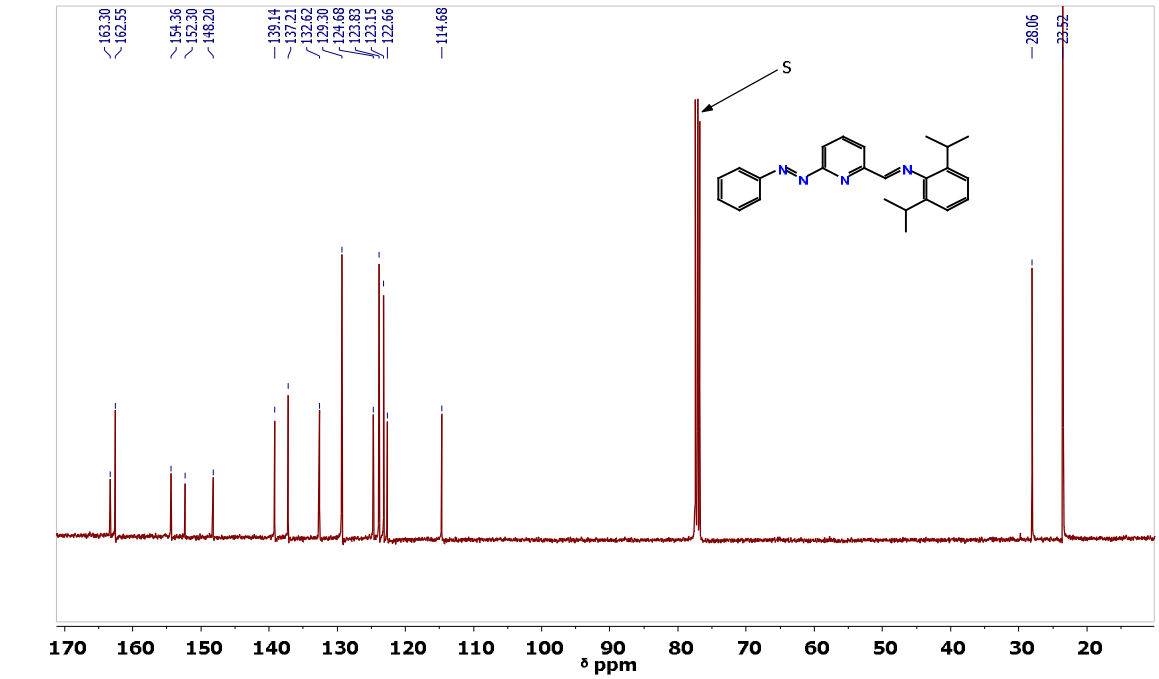

Figure S23. ^{1}H NMR Spectrum of **L^{x}** in $CDCl_3$.

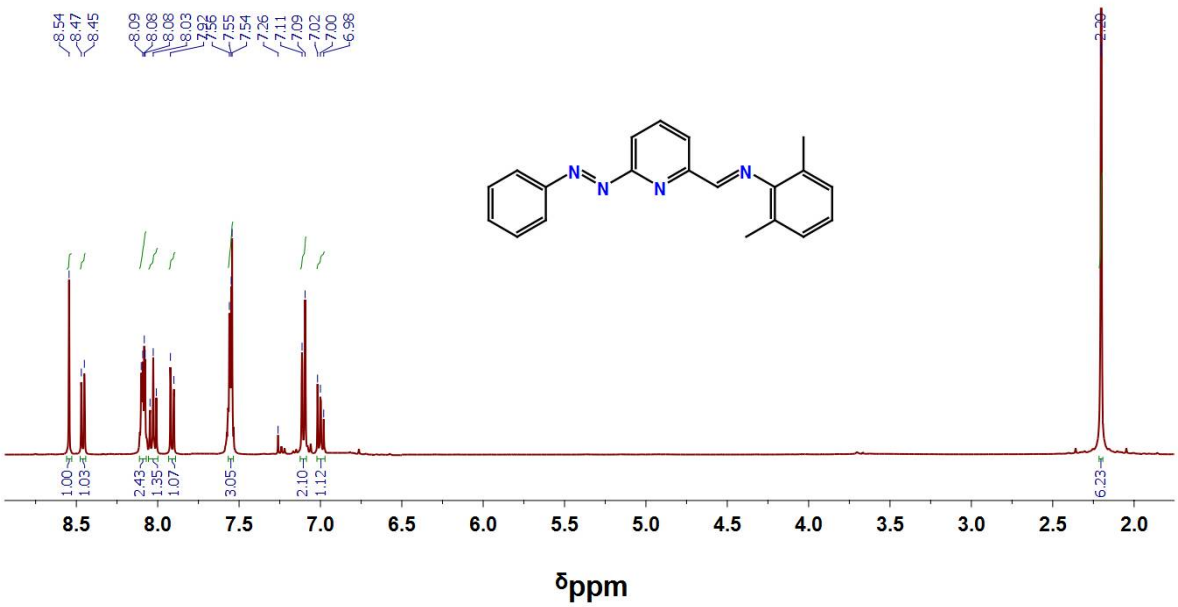

Figure S24. ^{13}C NMR Spectrum of **L^{x}** in $CDCl_3$.

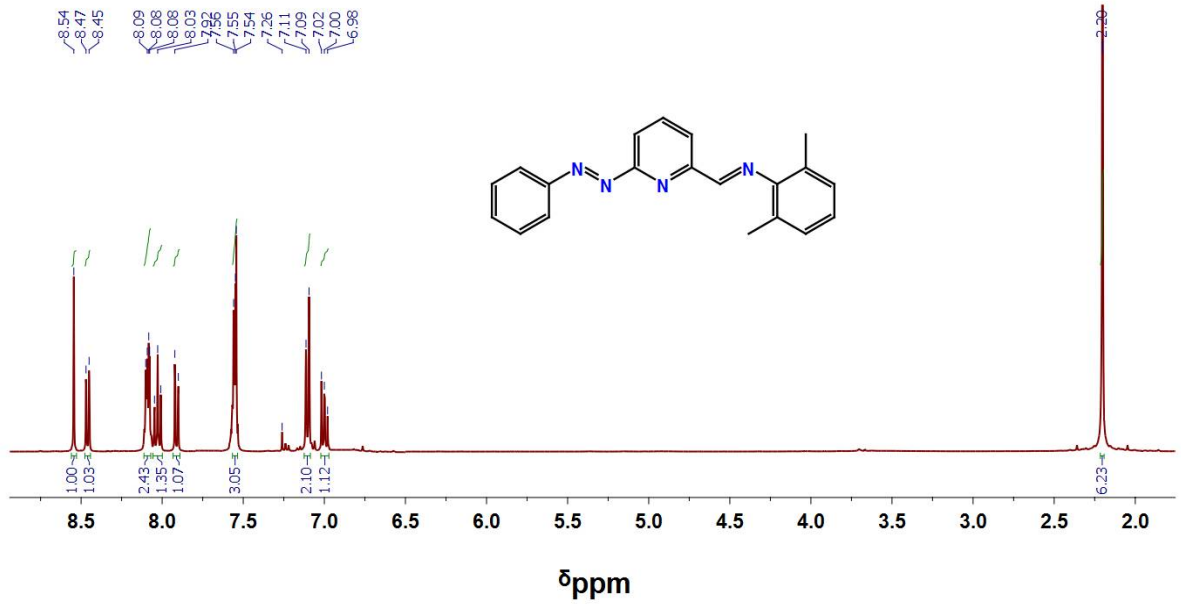

Figure S25. ^{1}H NMR Spectrum of **L^{y}** in $CDCl_3$.

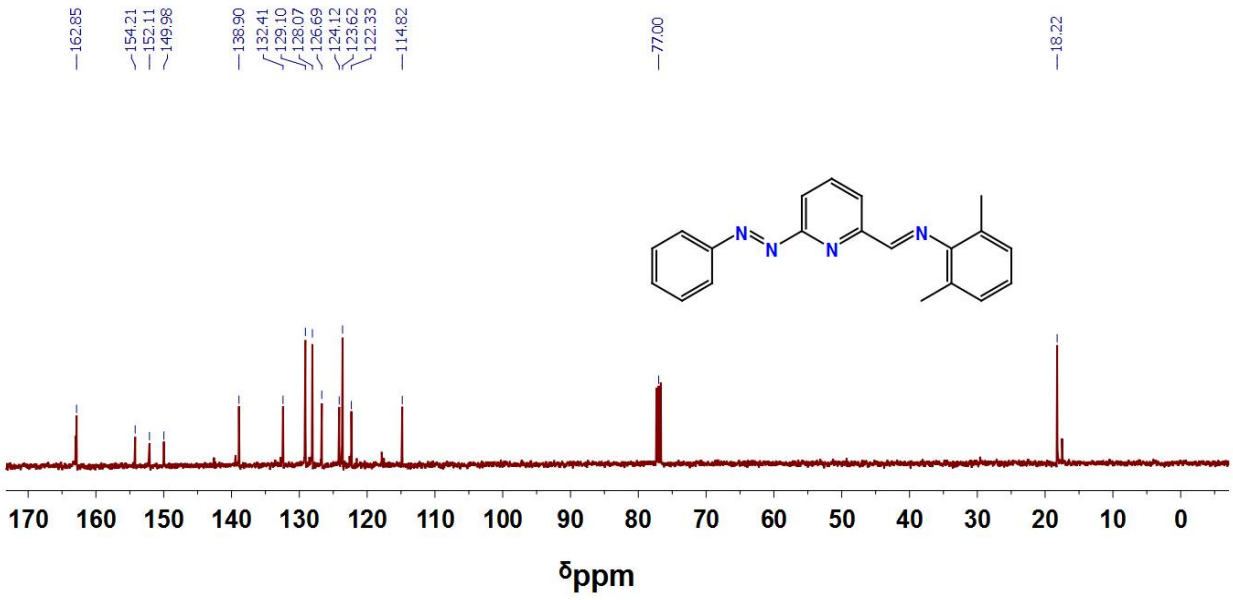

Figure S26. ^{13}C NMR Spectrum of **L^{y}** in $CDCl_3$.

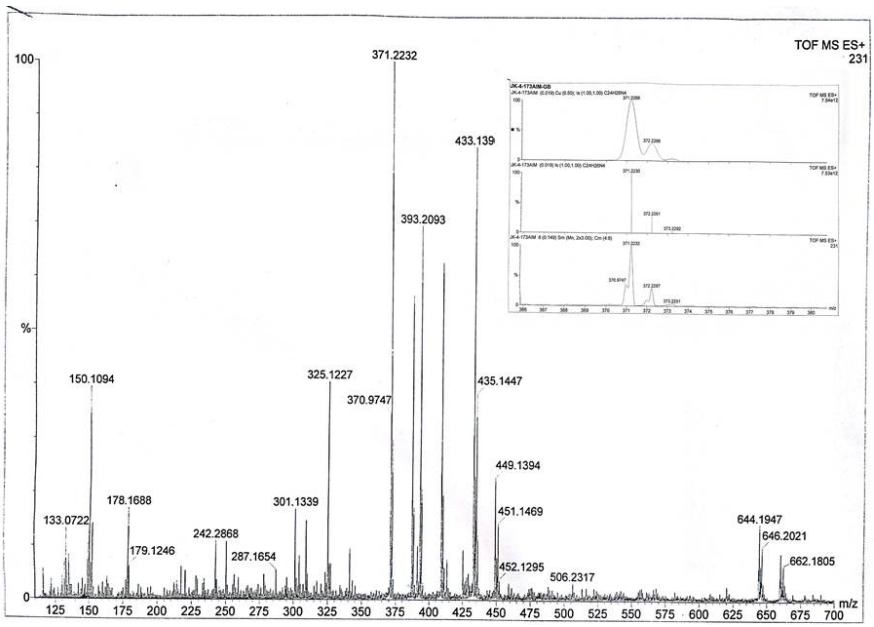

Figure S27. Full-range ESI-MS Spectrum of the ligand $\mathbf{L^x}$ in acetonitrile.

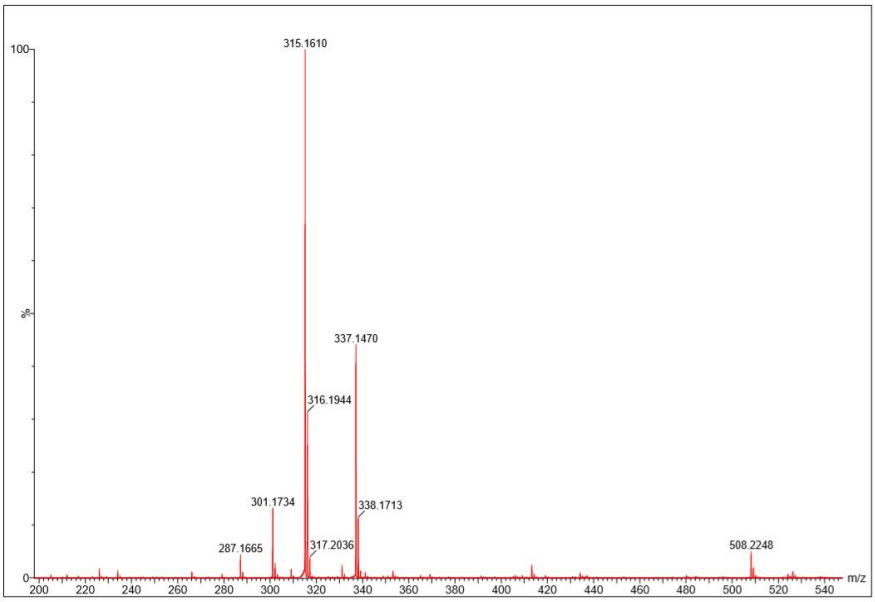

Figure S28. Full-range ESI-MS Spectrum of the ligand $\mathbf{L^y}$ in methanol.

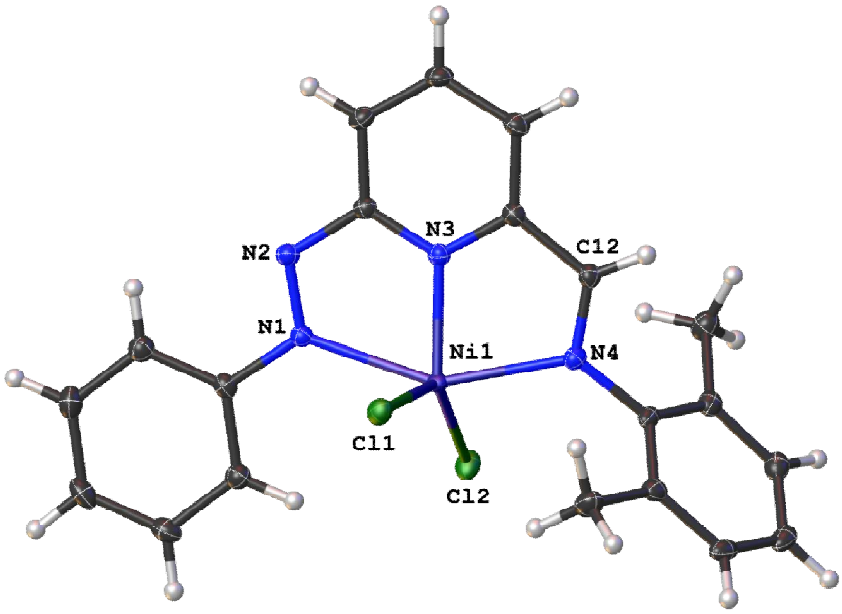

Figure S29. ORTEP representation and atom numbering schemes for the complex **8** in the 50% probability level.

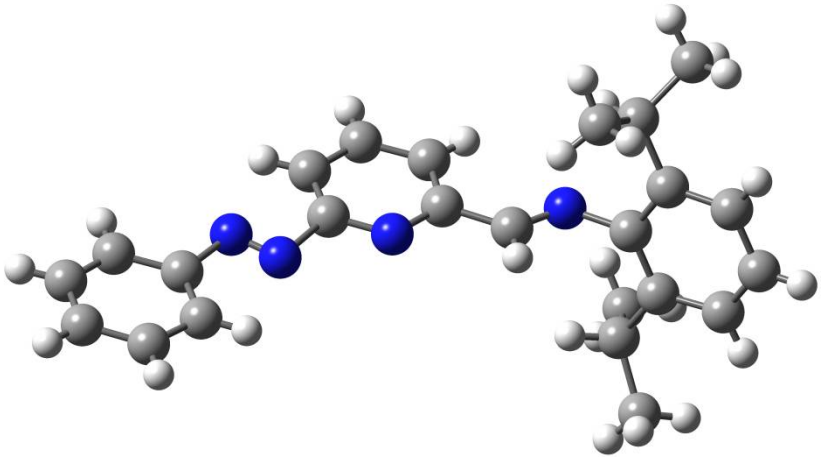

Figure S30. Optimized structure of the ligand $\mathbf{L^x}$

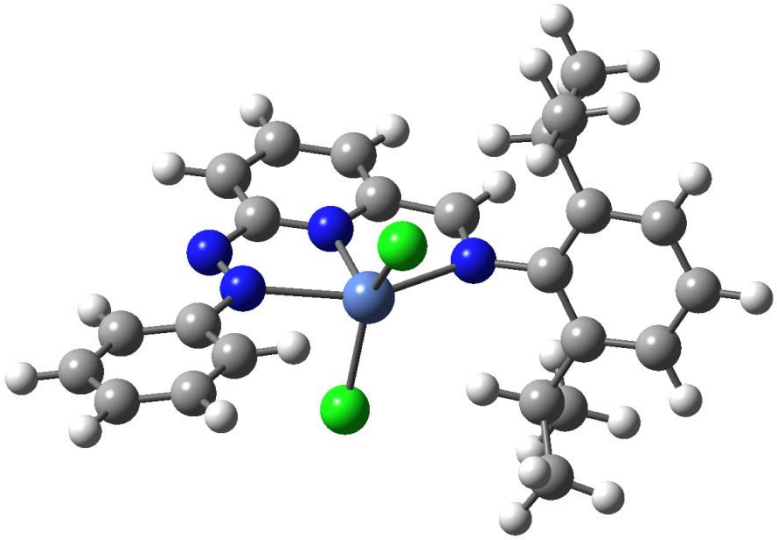

Figure S31. Optimized structure of Complex **7**

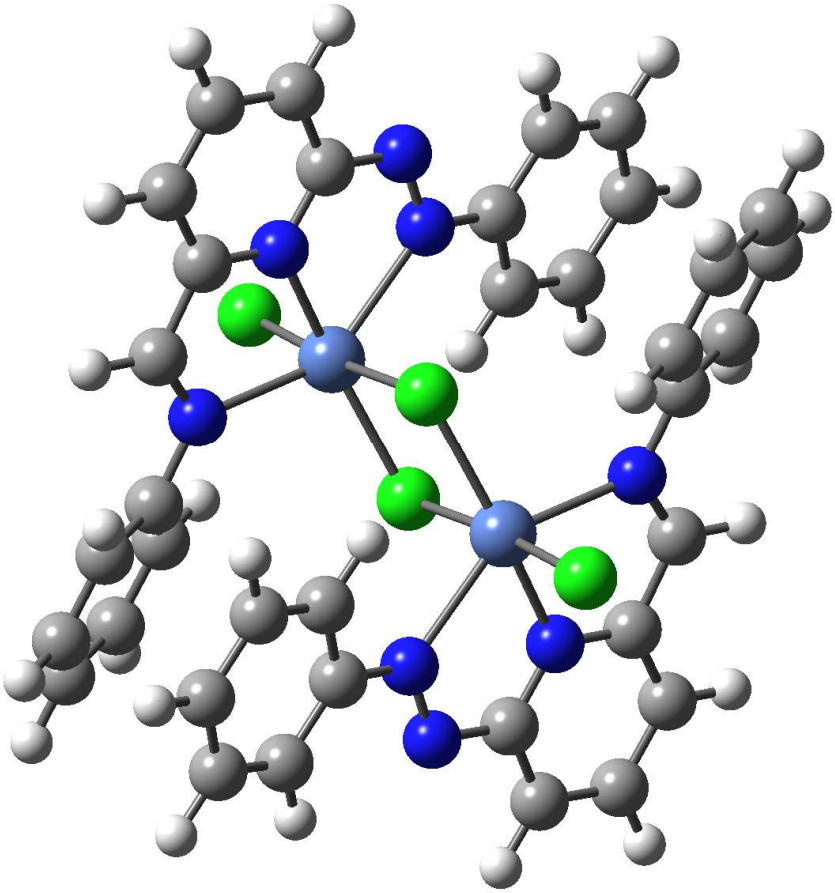

Figure S32. Optimized structure of Complex **9**

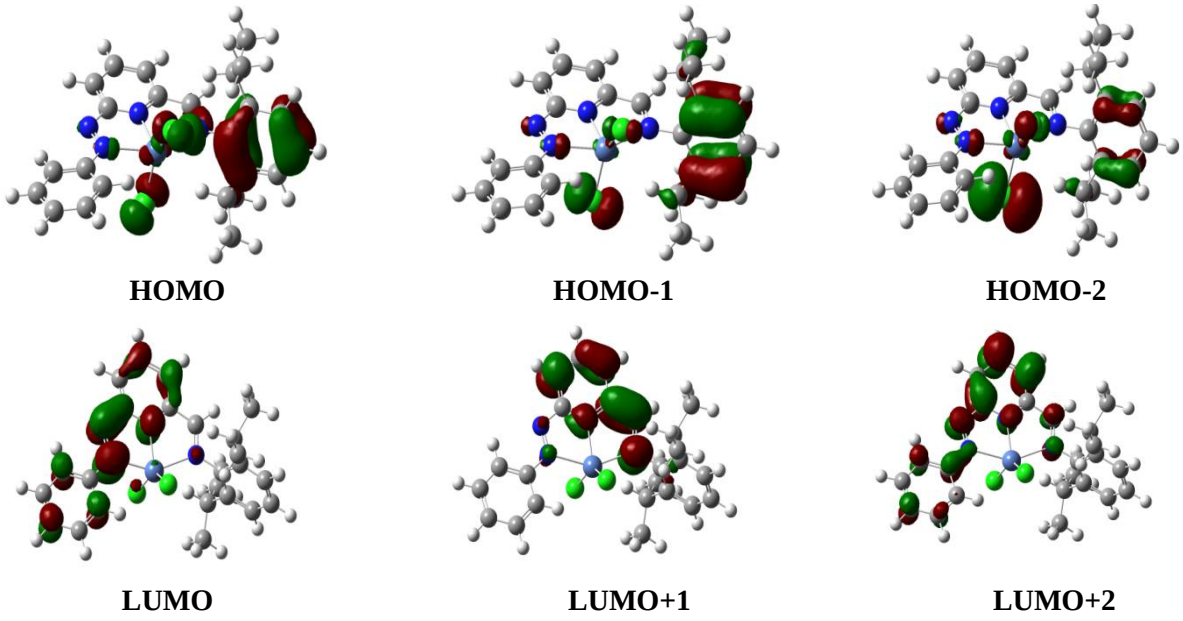

Figure S33: α-MOs of the Complex **7.**

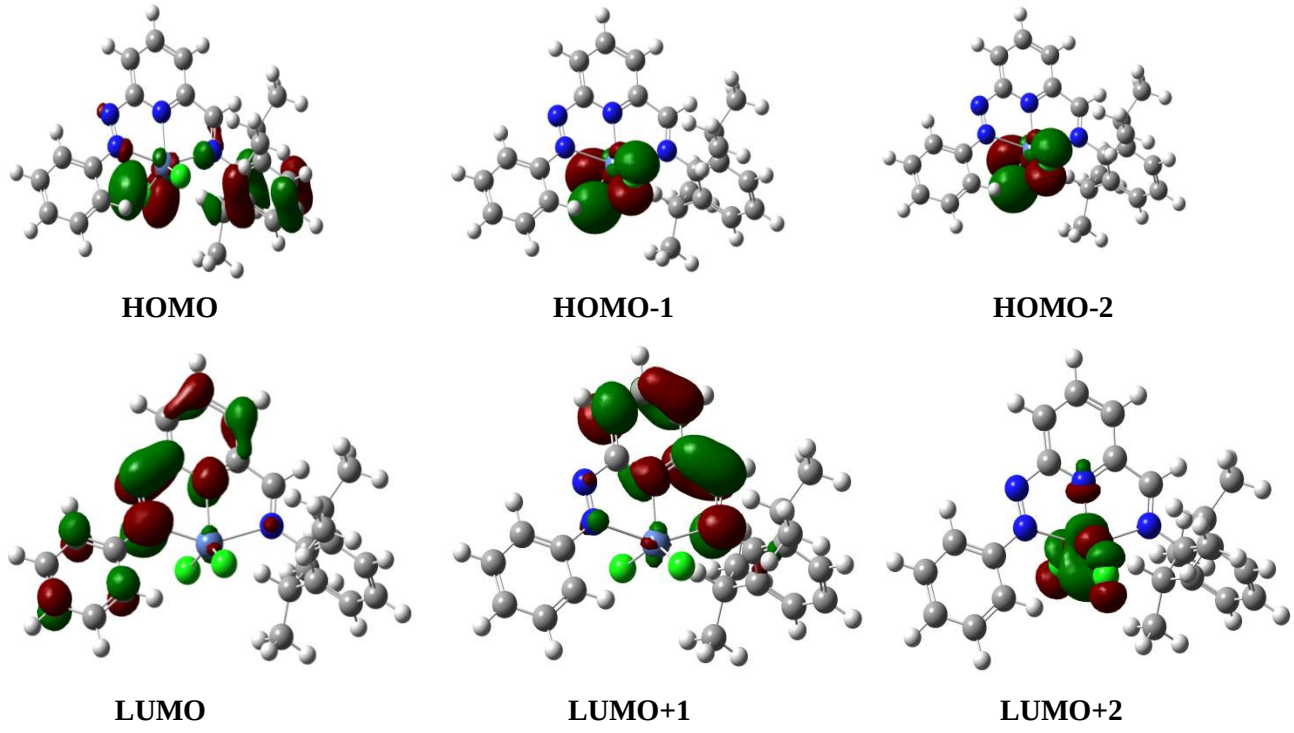

Figure S34: β-MOs of the Complex **7.**

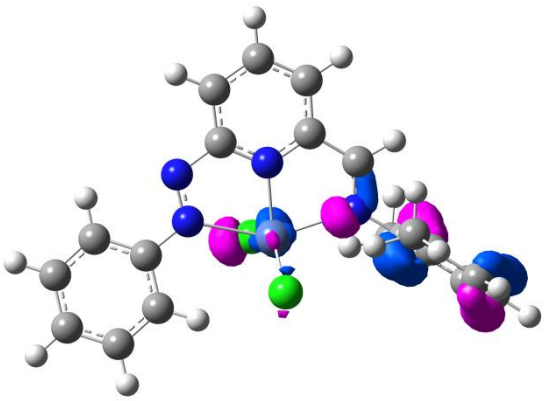

HOMO

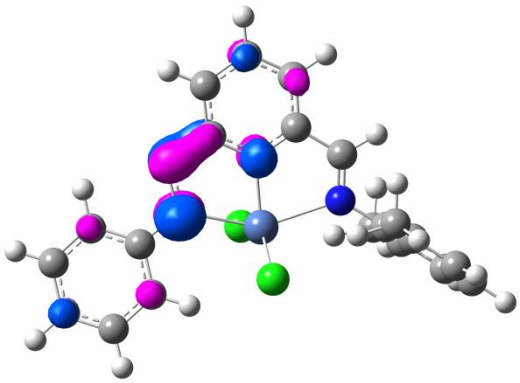

LUMO

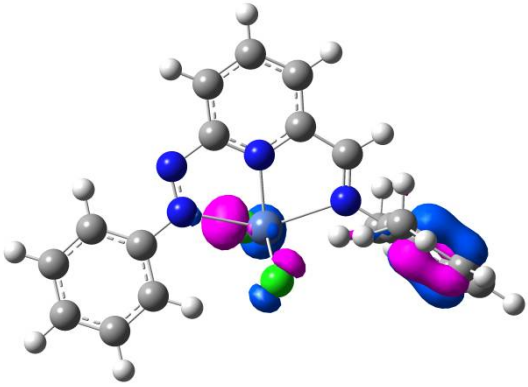

HOMO-1

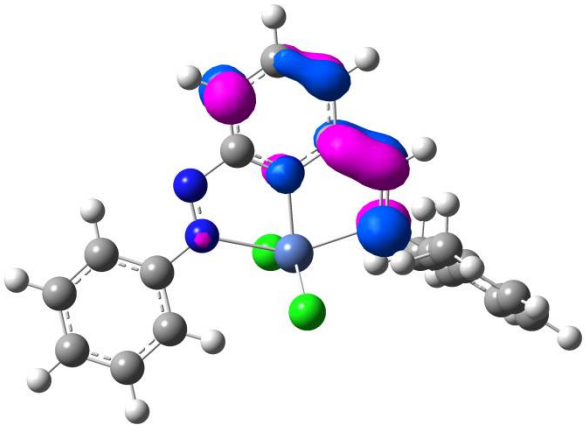

LUMO+1

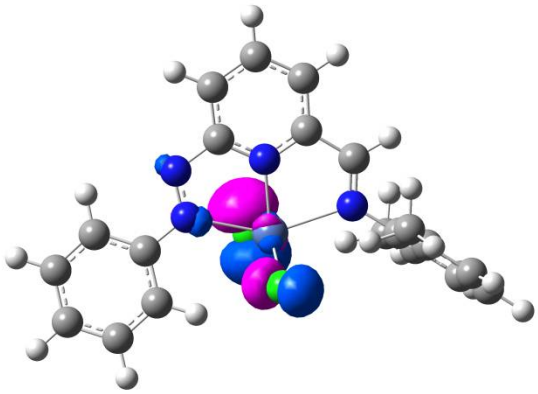

HOMO-2

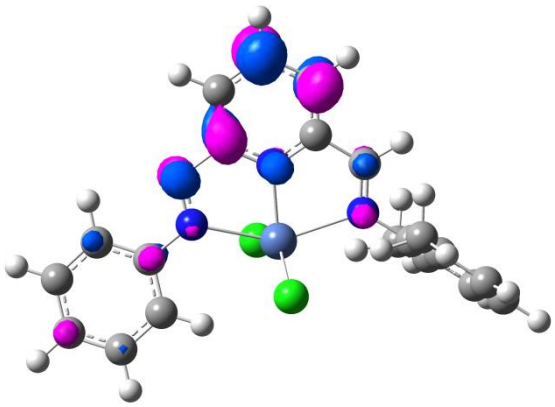

LUMO+2

Figure S35: α-MOs of the Complex **8.**

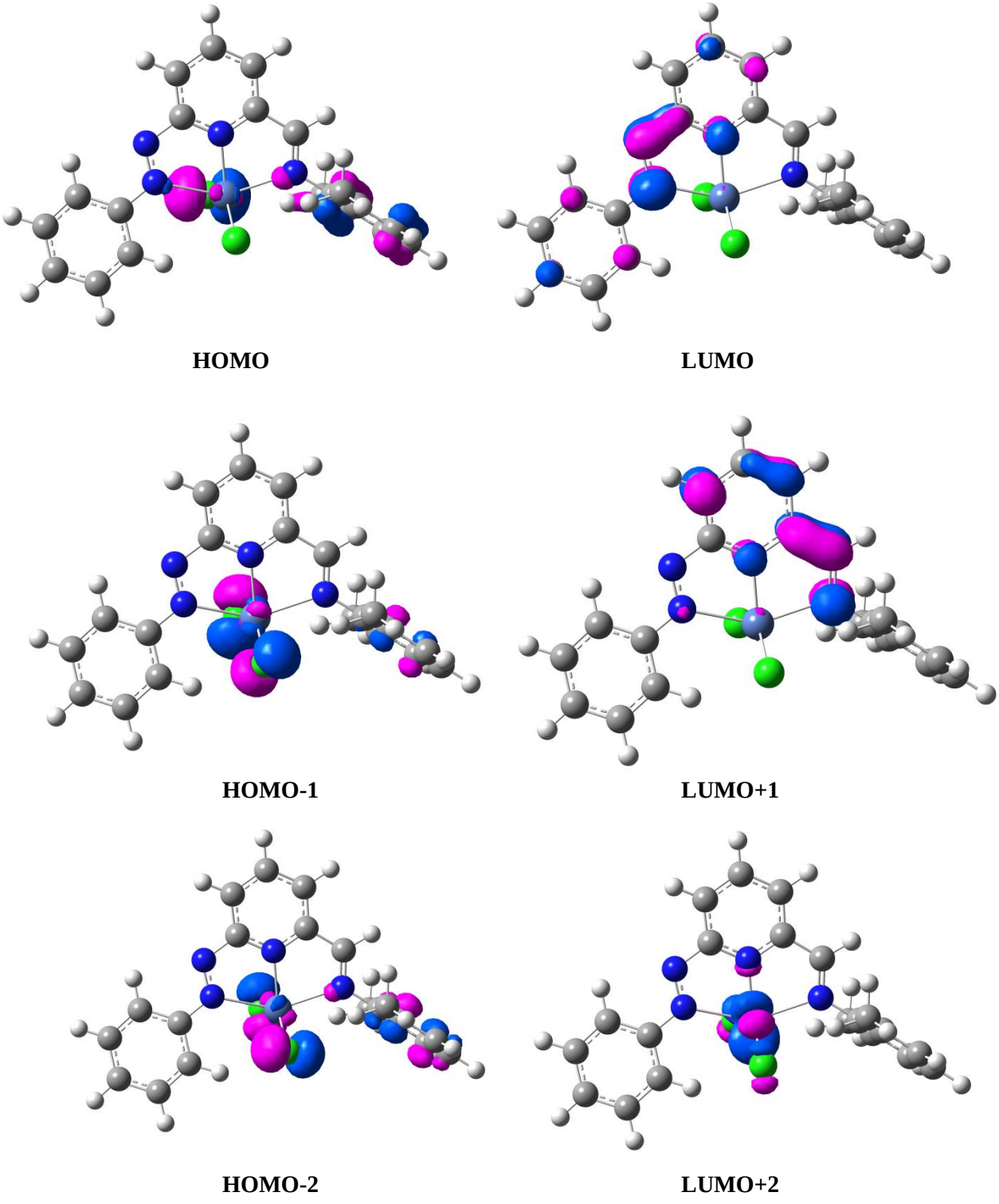

Figure S36: β-MOs of the Complex **8.**

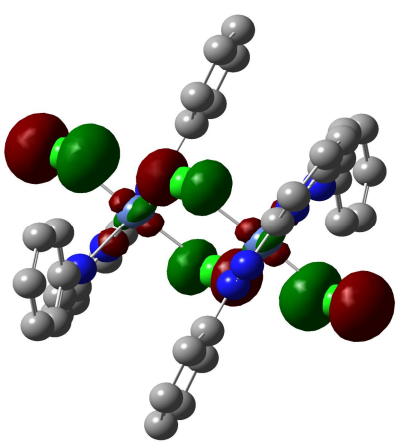

HOMO

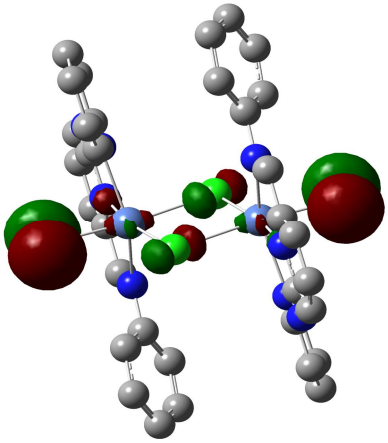

HOMO-1

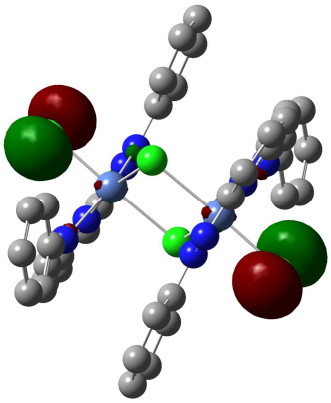

HOMO-2

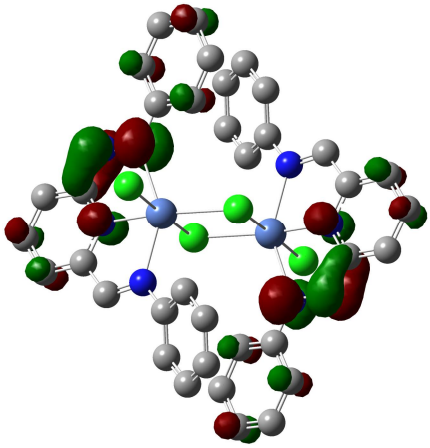

LUMO

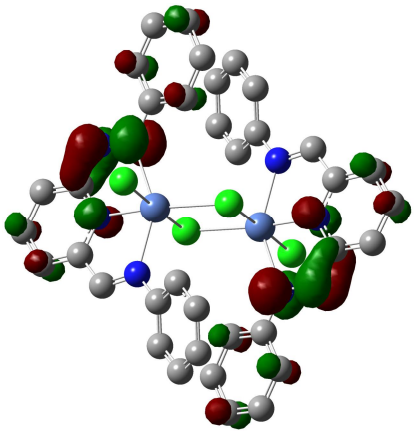

LUMO+1

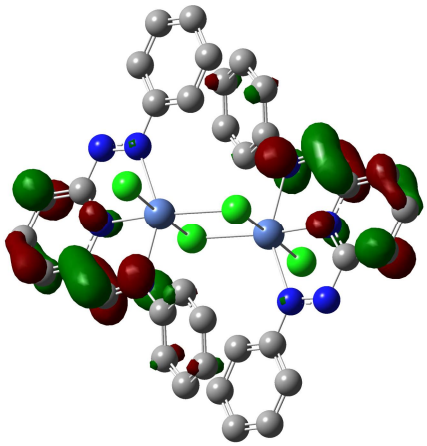

LUMO+2

Figure S37: α -MOs of the Complex **9.**

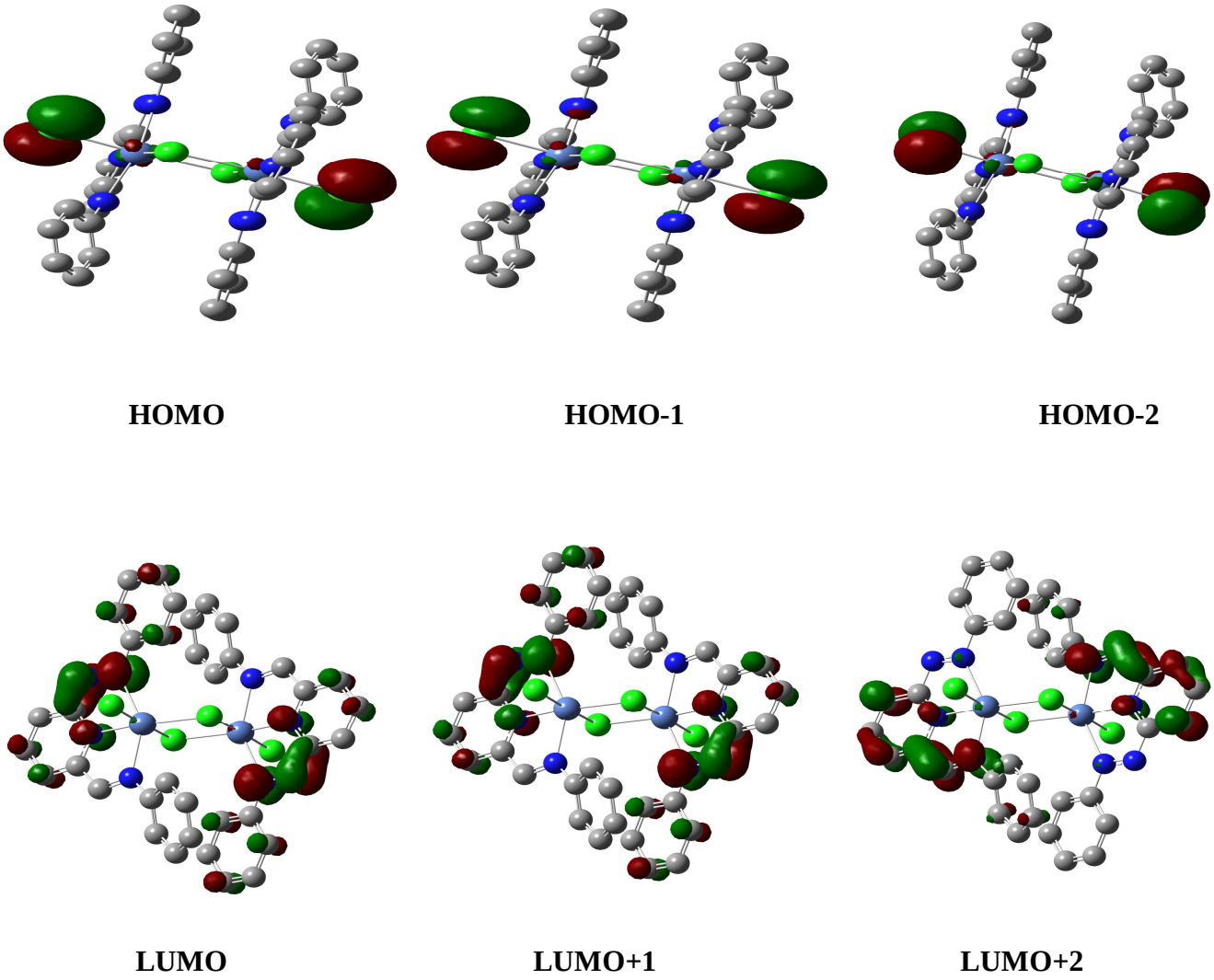

Figure S38: β -MOs of the Complex **9.**

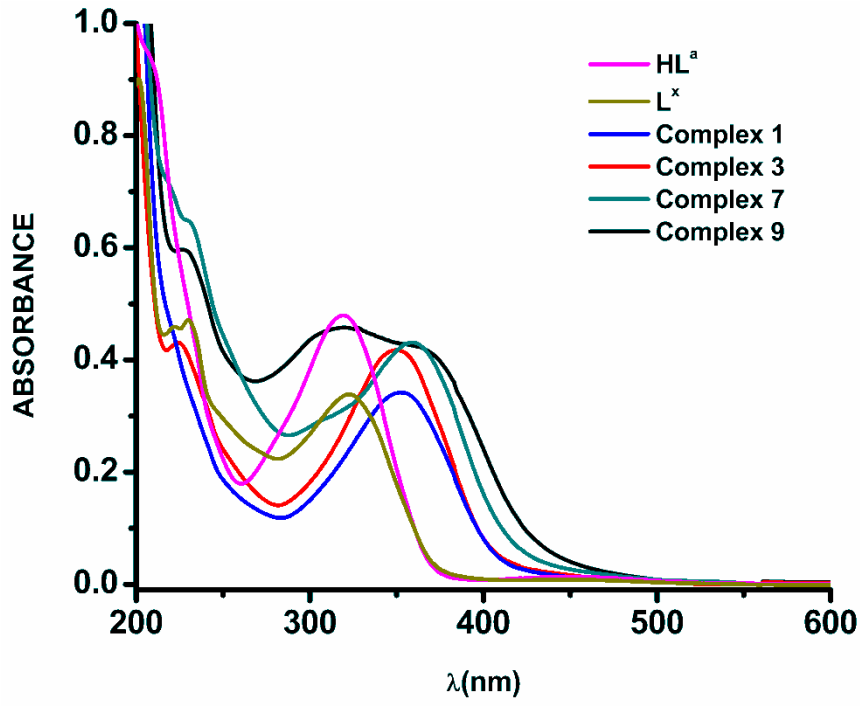

Figure S39: UV-vis spectra of **HL^a**, **L^x** and complex **1, 3, 7** and **9.**

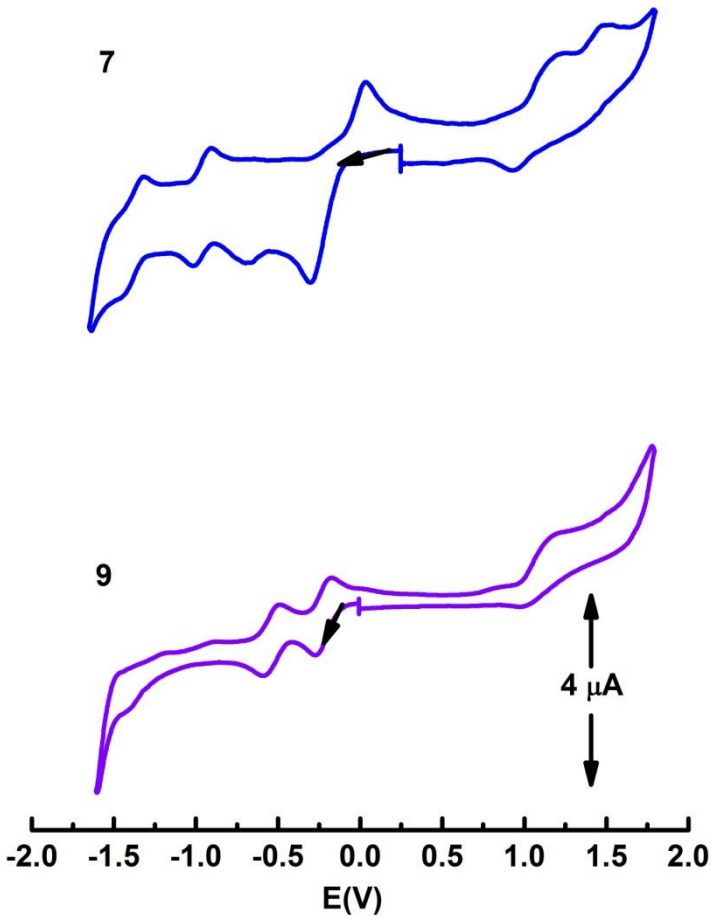

Figure S40. Cyclic voltammogram of the complex **7** and **9** in acetonitrile.

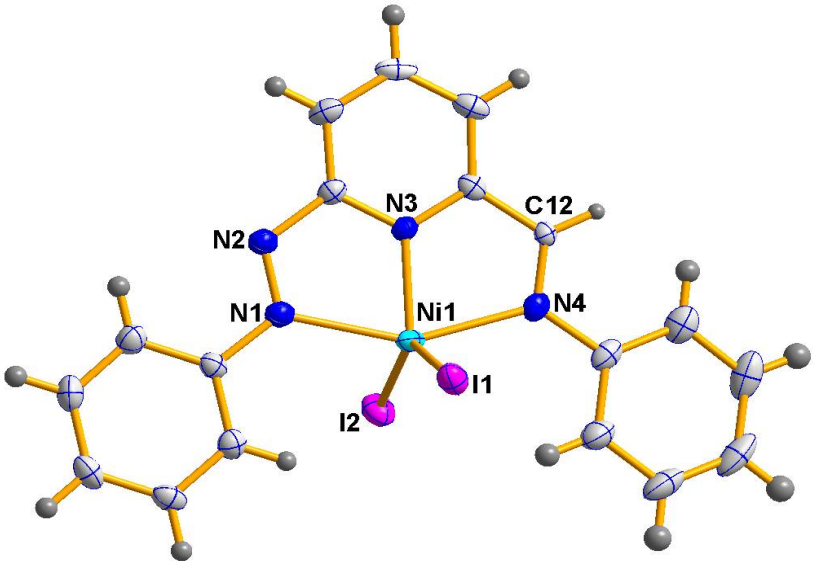

Figure S41. ORTEP representation and atom numbering schemes for the complex **10** in the 50% probability level.

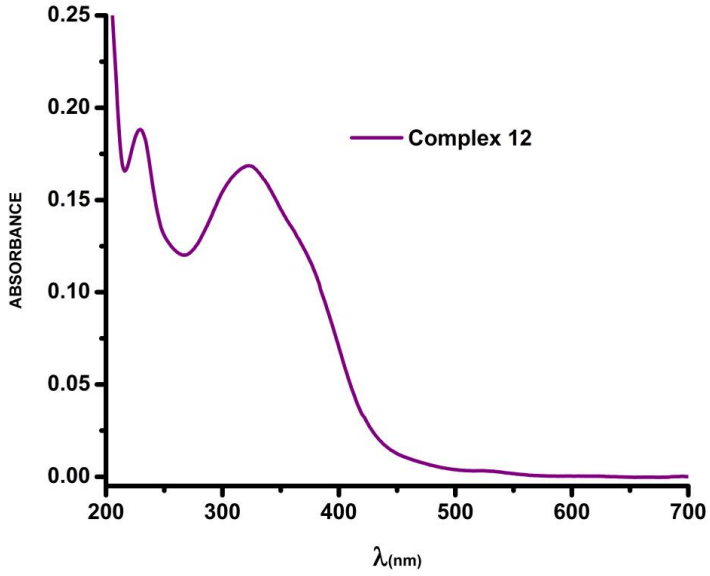

Figure S42. UV-vis spectra of the complex **12** in CH_3CN.

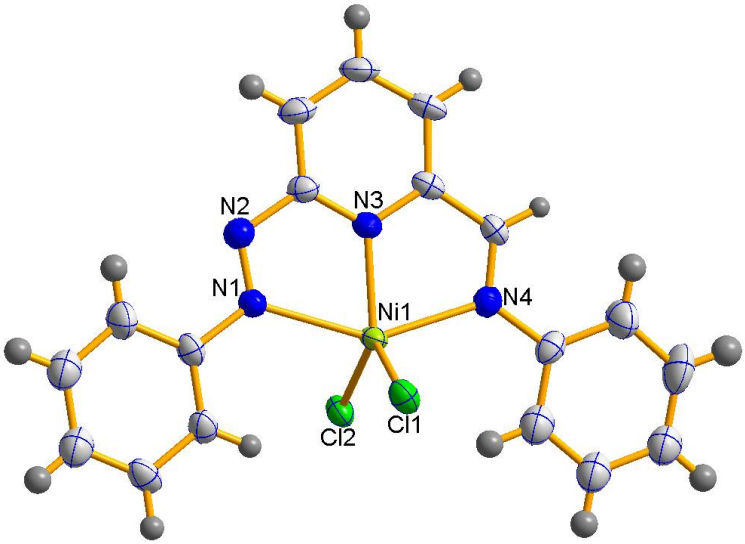

Figure S43. ORTEP representation and atom numbering schemes for the complex **12** in the 50% probability level.

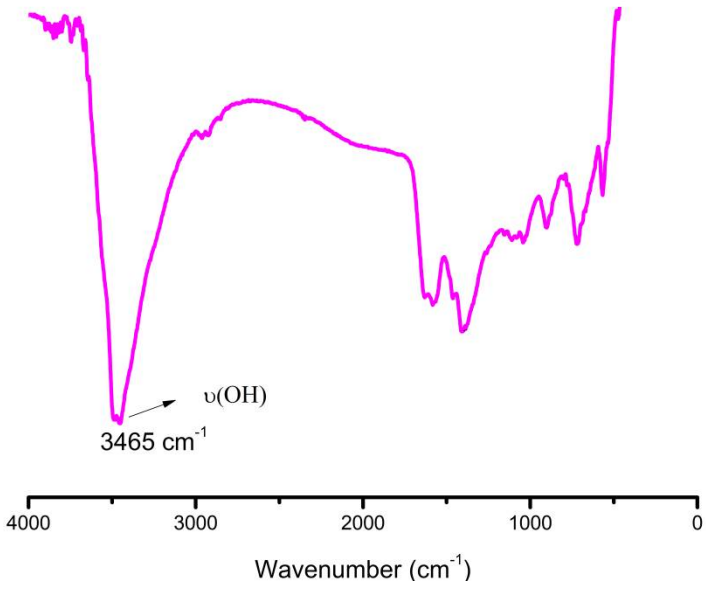

Figure S44: IR Spectrum of **$Zn(OH)_2$.**

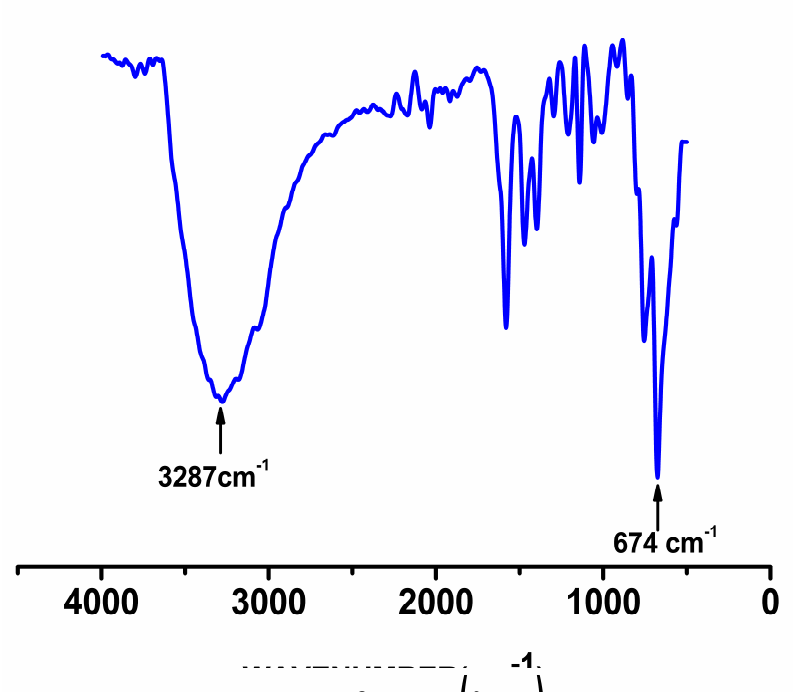

Figure S45: IR Spectrum of **[Cp_2Co]OH.**

Table S1. Crystallographic Data Table of the Complexes 2, 8, 10, and 12.

	2	**8**	**10**	**12**
CCDC no.	1887736	1964891	1887741	1887743
empirical formula	C_{20} H_{20} Cl_2 N_4 Ni	$C_{20}H_{18}Cl_2N_4Ni$	C_{18} H_{14} I_2 N_4 Ni	$C_{18}H_{14}Cl_2N_4$ Ni
formula wt.	445.99	443.99	598.82	415.92
crystal system	Triclinic	Orthorhombic	Monoclinic	Orthorhombic
space group	P-1	Pbca	$P2_1/n$	P b c a
a (Å)	9.0074(*5*)	13.3625(2)	10.3761(6)	13.7101(8)
b (Å)	9.9859(*6*)	14.1391(2)	15.2932(9)	14.8189(6)
c (Å)	11.7946(*6*)	20.0908(2)	11.9597(7)	17.3058(8)
α (deg)	87.050(*4*)	90.00	90.00	90.00
в (deg)	75.671(*5*)	90.00	95.1020(10)	90.00
γ (deg)	71.025(*5*)	90.00	90.00	90.00
Cell Volume	971.54(10)	3795.83(9)	1890.29(19)	3516.0(3)
R-factor	5.66	2.71	2.88	3.58
Z	2	8	4	8
T (K)	100.00(10)	100.00(10)	293.15 (10)	100.00(10)
μ (mm^{-1})	4.064	4.161	4.301	1.415
ρ_{calcd}($g\ cm^{-3}$)	1.525	1.554	2.104	1.572
F (000)	460.0	1824.0	1136.0	1696.0
2ϑ range (deg)	7.74 to 132.5	10.12 to 132.42	4.34 to 50.00	4.68 to 52.74
Data/restraints/ parameters	3350/0/250	3308/0/246	3321/0/220	3598/0/226
R_1, $wR_2[I >= 2\sigma(I)]$	0.0566,0.1561	0.0271, 0.0747	0.0288,0.0694	0.0358,0.0894
R_1, wR_2 (all data)	0.0581,0.1580	0.0281, 0.0755	0.0322,0.0709	0.0470,0.0976
GOF on F^2	1.062	1.057	1.127	1.056
largest difference in peak and hole(e $Å^{-3}$)	0.93,-0.99	0.27/-0.35	0.73,-0.75	0.40,-0.32